

Internal Stress in Nickel Thin Films Electrodeposited by a Rectangular Current Pulse Technique

M. Saitou

Department of Mechanical Systems Engineering, University of the Ryukyus, 1 Senbaru Nishihara-cho Okinawa, 903-0213, Japan

*E-mail: saitou@tec.u-ryukyu.ac.jp

Received: 8 April 2015 / Accepted: 12 May 2015 / Published: 27 May 2015

A scaling behavior of the internal stress in a nickel thin film electrodeposited by a rectangular current pulse technique was investigated using a bent strip measurement. The internal stress that appears as a tensile stress is found to obey a scaling law represented by power laws of the film thickness and the Faradaic current pulse amplitude in one period. An increase in the film thickness combined with the fluctuation of the surface roughness in a statistical surface growth model decreases the internal stress. A decrease in the Faradaic current pulse amplitude that indicates a number of nickel ions arriving at the electrode in one period lessens the internal stress owing to an increase in the mean grain size. The scaling behavior of the internal stress suggests that the internal stress links the surface topography.

Keywords: internal stress; rectangular current pulse technique; scaling law; nickel thin film

1. INTRODUCTION

The internal stress [1-2] in thin films deposited on substrates has been investigated experimentally and theoretically. One of the goals for the experimental studies is to describe the internal stress using experimental parameters, however, the influences of many parameters on the internal stress are so complicated that, for example, the internal stress that emerges in the thin film changes from a compressive stress to a tensile stress depending on the parameter [3-4].

On the other hand, scaling is an important concept in modern statistical physics [5], especially in phase transitions. Scaling is often described by simple power laws having exponents that determine universality classes characterizing the scaling behavior, irrespective of experimental details. In film growth, statistical surface growth models [6] using the scaling hypothesis have a feature that the scaling exponent is independent of the experimental details. The internal stress occurs during film

growth that is well described by the statistical surface growth model [7]. Hence, the internal stress is also expected to obey the scaling law. The goal of our study is to enable us to describe the complicated behavior of the internal stress with the help of the scaling approach.

A rectangle current pulse technique in electrodeposition [8], which has advantages of three parameters varied independently, i.e., the current pulse amplitude, an on-time of the current, and an off-time of the current, is often used for a study on the effect of the three parameters on the internal stress in electrodeposits [9-10]. In addition, as the electric double layer formed between an electrode and solution has a capacitative property, a portion of the rectangle current pulse passes through the electric double layer as a non-faradaic current that does not contribute to the formation of films at the electrode [11]. Hence, the effect of the pulse current amplitude on the internal stress should take into consideration the non-faradic current.

In this study, Ni electrodeposition from a nickel sulfamate solution was chosen because it has almost 100% current efficiency in direct current electrodeposition. The bent strip measurement [12], which is one of the curvature measurement methods, was applied to measure the internal stress in nickel thin films. The two-legged beryllium copper strips whose opposite sides are electrodeposited causes the leg deflection from which the internal stress is calculated.

A Williamson-Hall technique in X-ray diffraction (XRD) was applied [13-14] to determine a mean grain-size in the nickel film. The conventional Williamson-Hall technique assuming the uniform deformation is based on the Bragg peak broadening due to the grain-size and strain in the film. Hence, several Bragg diffraction peaks are required to estimate the mean-grain size. In a modified Williamson-Hall technique considering anisotropic deformation [14], Young's modulus, stress, and strain are dependent on the Miller indices. The Bragg diffraction broadening in the electrodeposited Ni thin film, which in this study is well described by the conventional Williamson-Hall technique, will be analyzed.

In the present study, we demonstrate that the internal stress in the nickel films deposited by the rectangular current pulse electrodeposition technique obeys the simple power law.

2. EXPERIMENTAL SET UP

2.1 Rectangular current pulse electrodeposition

The experimental procedure for the bent strip measurement [12] was as follows: A test specimen (Specialty Testing and Development Co. made) consisting of two legs made of beryllium copper was prepared for a cathode electrode. One side of the leg was coated with an insulating organic thin film to prevent electrodeposition. Two poly-crystalline nickel sheets of 90x60x0.5 mm³ were prepared for anode electrodes.

The cathode and two anode electrodes were put in a quiescent bath containing (gL⁻¹): nickel sulfamate 600 and boric acid 40. The cathode electrode was located in the center of the two anode electrodes. The bath was maintained at pH 4 and a temperature of 298 K. The rectangle current pulse having an amplitude of 5 to 129 mA cm⁻², an on-time of the current ranging from 2 to 20 ms, and an

off-time of the current ranging from 1 to 20 ms were provided with a bipolar power supply (Advantest 6241A) as a constant current source to deposit nickel on each bare side of the two legs. The main merit of the bipolar power supply with fast output response (for example, a rise time less than 600 μ s and a fall time less than 30 μ s) is to supply the rectangular pulse current without any distortion of the waveform irrespective of the impedance in the electrochemical cell.

After electrodeposition, the test specimen was rinsed with distilled water and dried. Changes in both the curvature and the weight of the test specimen were measured to determine the internal stress.

2.2 Current efficiency in rectangular current pulse electrodeposition

The hydrogen evolution usually takes place in electrodeposition. So as to avoid the hydrogen evolution in nickel electrodeposition, in this study, the nickel sulfamate solution was chosen because it has almost 100% current efficiency in direct current electrodeposition.

The current efficiency is defined by the normalized mass deposit that means the ratio of the mass of metal actually deposited on the electrode to the deposited mass if all the current is used for deposition. In our experiment, the current efficiency of nickel films formed by a direct current technique was about 99 % using the nickel sulfamate solution. However, in current pulse electrodeposition, the capacitative behavior of the electric double layer formed between the electrode and solution causes the non-faradic current that just only passes through the electric double layer.

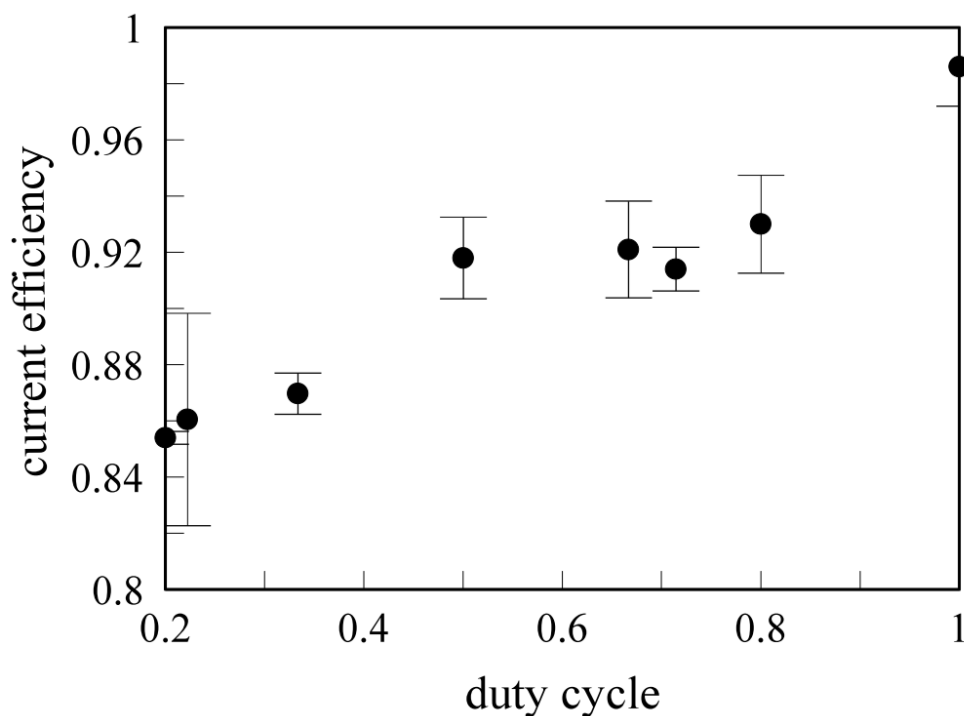


Figure 1. A plot of the current efficiency vs. the duty cycle in rectangular pulse current electrodeposition. The current efficiency at the duty cycle of 1 indicates that in direct current electrodeposition.

A plot of the current efficiency vs. the duty cycle under the experimental conditions above-stated is shown in Fig. 1. A decrease in the current efficiency in rectangular current pulse electrodeposition is caused not by the evolution of hydrogen, but by the capacitive characteristic of the electric double layer. Hence, the internal stress in this study has no relationship with the hydrogen gas. In addition, the faradaic current subtracted the non-faradaic current from the total current is obtained from Fig. 1.

2.3 Estimate of the mean grain size using XRD

The nickel thin film electrodeposited on the test specimen was investigated to obtain the mean grain size by conventional XRD (Rigaku Ultima) with $\text{CuK}\alpha$ radiation using a standard θ - 2θ diffractometer with a monochromator of carbon.

3. EXPERIMENTAL RESULTS AND DISCUSSION

3.1 Power law of film thickness

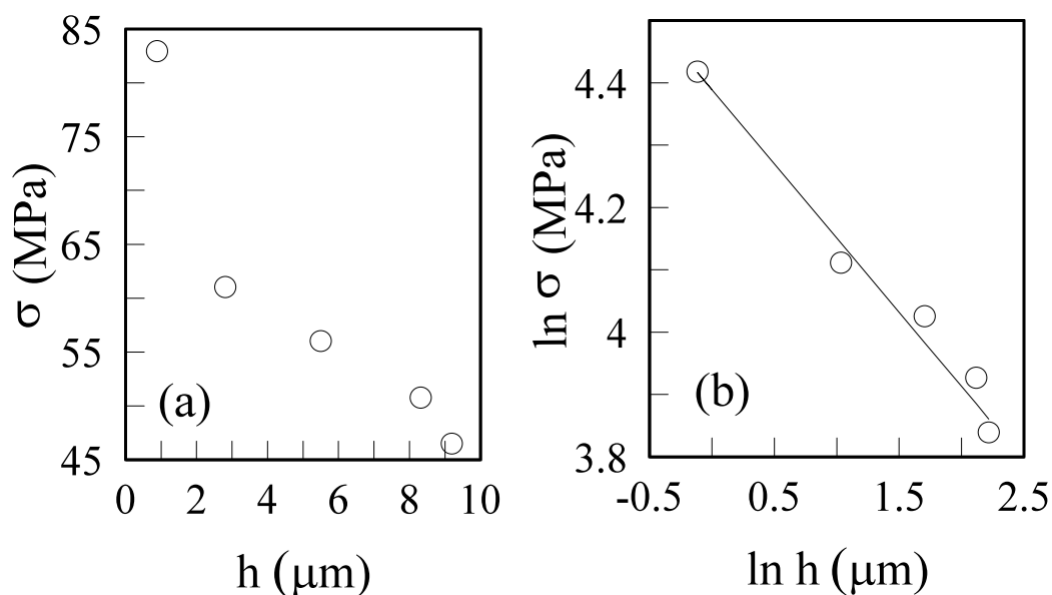


Figure 2. Internal stress in the nickel thin film electrodeposited at a current pulse amplitude of 25 mA cm^{-2} , an on-time of 5 ms, and an off-time of 5 ms. (a) Dependence of the internal stress on the film thickness. (b) A log-log plot of the internal stress vs. the film thickness. The slope best fitted to the data yields 0.24 ± 0.02 .

Figure 2 (a) shows that the internal stress in the nickel film electrodeposited at a rectangular current pulse amplitude of 25 mA cm^{-2} , an on-time of 5 ms, and an off-time of 5 ms decreases with the film thickness. Figure 2 (b) shows that the internal stress σ obeys a power law of film thickness h ,

$\sigma \sim h^{-0.24 \pm 0.02}$. Jassen et al. [15] reported $\sigma \sim h^{-0.22}$ for CrN thin films formed by reactive sputter deposition.

The correlation length ξ that means the spatial extent of fluctuations in a physical quantity such as the surface roughness obeys a power law [6],

$$\xi \sim h^{1/z}, \tag{1}$$

where z is called the dynamic exponent that describes the scaling of a relaxation times with the system size. Here the relaxation time is defined as the time for the surface roughness to saturate. On the other hand, a grain boundary relaxation model [1-2] predicts an inverse dependence of the internal stress on a mean grain size d . As the correlation length is considered to be comparative in size to the mean grain size d , the internal stress becomes

$$\sigma \sim d^{-1} \sim h^{-1/z}. \tag{2}$$

Thus, the exponent in the power law of film thickness is interpreted as the reciprocal of the dynamic exponent, which is reported to have an experimental value [15] within a range from 0.22 to 0.79. In a statistical surface diffusion growth model [16], the dynamic exponent has a value of 4, which gives 0.25 as the reciprocal approximately equal to the exponent in this experiment. After the relaxation time, the internal stress is also considered to saturate. The surface topography such as the fluctuation of the surface roughness seems to link the internal stress [7].

3.2 Power law of the duty cycle

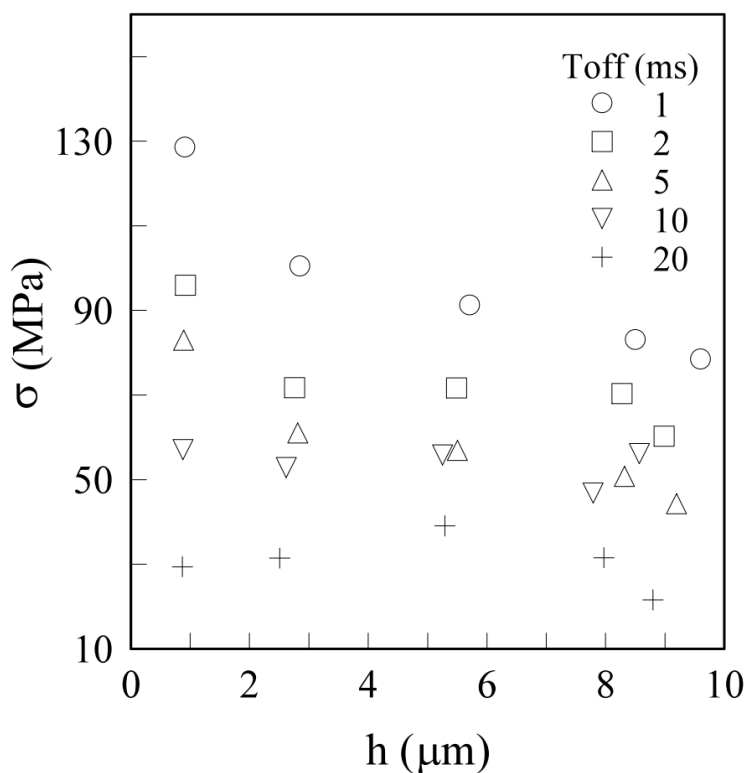


Figure 3. Internal stress in the nickel thin film electrodeposited at a current pulse amplitude of 25 mA cm⁻² and an on-time of 5 ms for five kinds of the off-time T_{off}.

The internal stress in the nickel film electrodeposited at a fixed current on-time of 5 ms is shown in Fig. 3. An increase in the off-time appears to lessen the internal stress that decreases with the film thickness.

In Fig. 4, the effect of the current on-time on the internal stress in the nickel film electrodeposited at a fixed current off-time of 5 ms is shown. An increase in the current on-time of the current appears to increase the internal stress.

According to Eq. (2), the internal stress determined by the film thickness is affected not by the off-time during which no film growth takes place, but by the duty cycle at which the nickel film is grown. Hence, the internal stress should be redrawn as a variable of the duty cycle as shown in Fig. 5. All the data in Figs. 3 and 4 almost lie on the straight line. The slope of the best straight line fitted to the data yields the exponent value of 0.74 ± 0.04 . Thus, we have

$$\sigma \sim h^{-0.24} \left(\frac{T_{on}}{T_{on} + T_{off}} \right)^{0.74} \quad (3)$$

The second term on the right hand side in Eq. (3) is required to include the current term from which the non-faradaic current is subtracted. The result in this study shows the scaling behavior similar to one in vapor growth [15]. This is because (1) in our study no additive such as NiCl [11] and saccharin [17] was used, (2) hydrogen evolution [18] was suppressed owing to the high current efficiency, and (3) according to the dynamic scaling theory the exponent n is independent of experimental details [6].

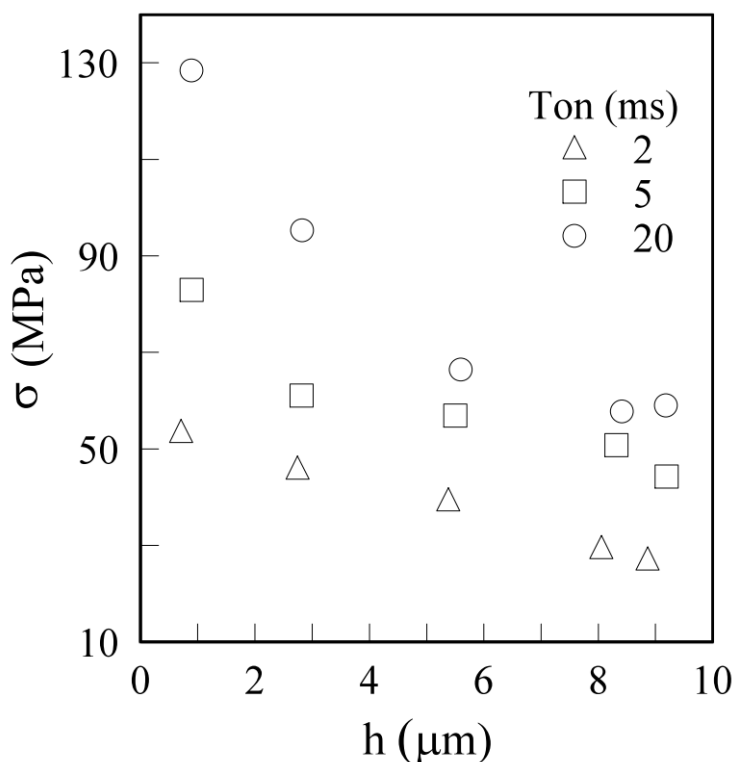


Figure 4. Internal stress in the nickel thin film electrodeposited at a current pulse amplitude of 25 mA cm^{-2} and an off-time of 5 ms for three kinds of the current on-time T_{on} .

3.3 Faradaic current in rectangular current pulse electrodeposition

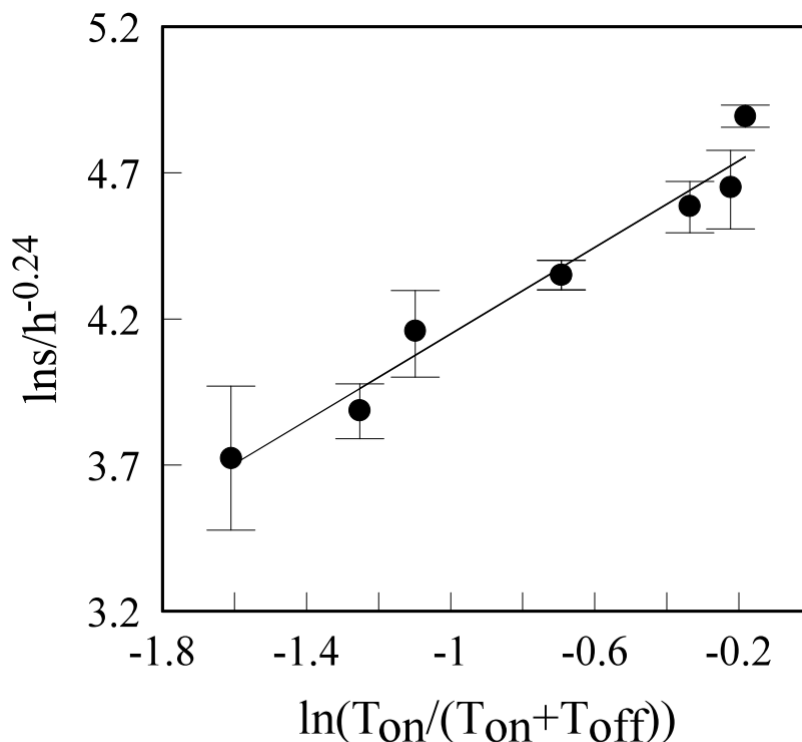


Figure 5. A log-log plot of $\sigma/h^{-0.24}$ vs. $T_{on}/(T_{on}+T_{off})$. All the data in Figs. 3 and 4 is plotted. The straight line best fitted to the data yields a slope of 0.74 ± 0.04 .

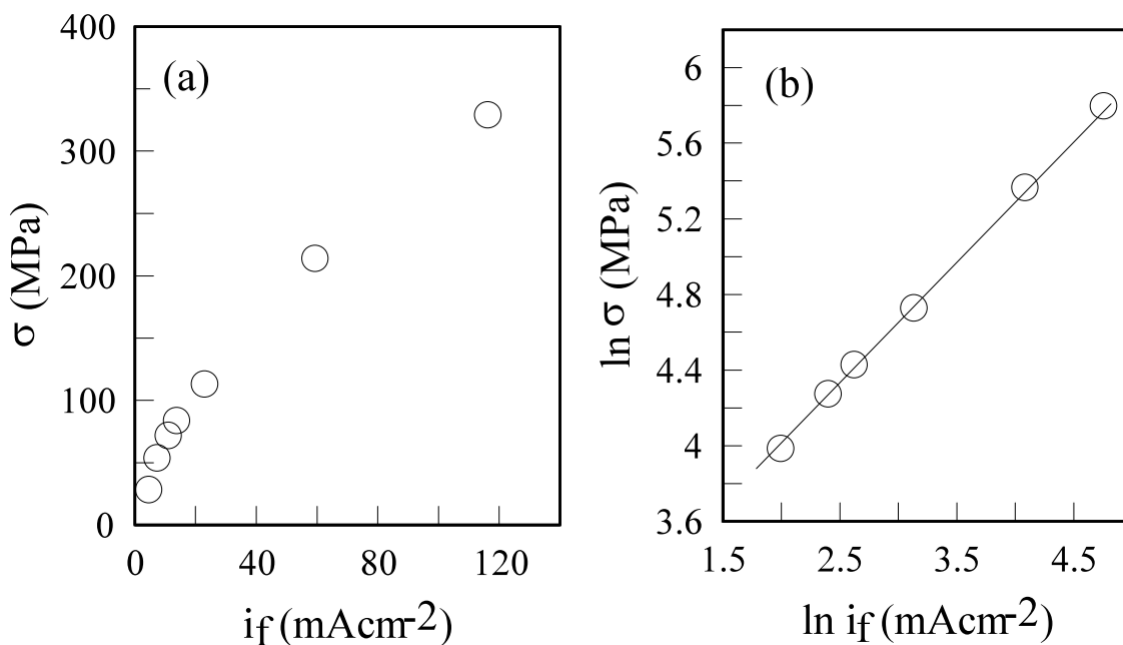


Figure 6. A plot of the internal stress vs. the Faradaic current pulse amplitude at a film thickness of 1.0 μm . The straight line best fitted to the data, gives the slope of 0.74 ± 0.01 .

The rectangular current pulse applied to the electrodes generates the non-faradaic current and the faradaic current. As the current consumed the formation of hydrogen is negligible small, the faradaic current is simply deduced from the current efficiency in Fig. 1. A plot of the internal stress vs. the faradaic current amplitude i_f is shown in Fig. 6 (a). The slope in Fig. 6 (b) yields the power-law relation,

$$\sigma \sim i_f^m, \tag{4}$$

where the exponent is 0.74 ± 0.01 . Thus, taking into consideration the non-faradaic current, we have the internal stress described by,

$$\sigma \sim h^{-0.24} \left[i_f \left(\frac{T_{on}}{T_{on} + T_{off}} \right) \right]^{0.74}. \tag{5}$$

The second term on the right hand side in Eq. (5) is interpreted as a number of nickel ions arriving at the electrode, which form grains in the nickel film. The scaling behavior indicates that the origin of internal stress relates the phase transition in growth. However, it is noted that some deviations from the simple scaling law are often observed owing to the presence of products incorporated into electrodeposits, for example, impurities that cause compressive stress [17, 20], grain texture [18], and some compounds [19] formed by electrochemical reactions. In this study, the experiments were performed to avoid the deviation.

3.4 Mean grain size determined by XRD

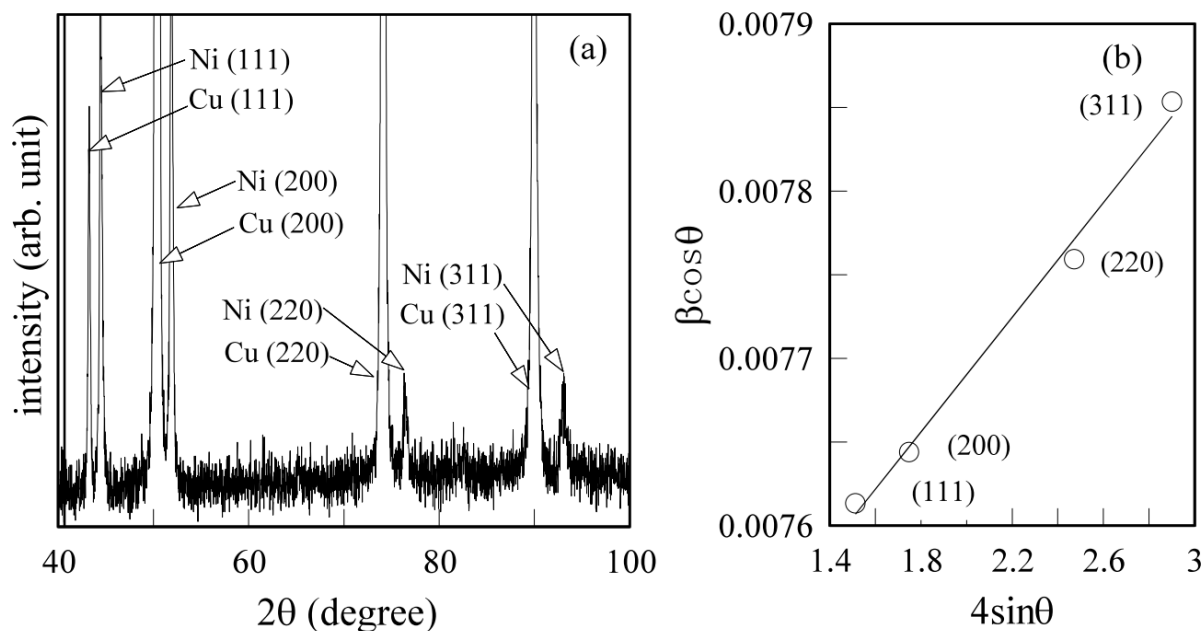


Figure 7. Typical XRD chart of the nickel thin film and Williamson-Hall plot for the nickel thin film of 1 μm in thickness. (a) The XRD chart of the nickel thin film electrodeposited at a current pulse amplitude of 25 mA cm^{-2} , an on-time of 5 ms, and an off-time of 5 ms. The diffraction peaks of the nickel thin film and copper substrate were observed. (b) The straight line best fitted to the line broadening coefficient of (111), (200), (220) and (311) yields the mean grain size of the nickel thin film.

Next, we examine the effect of i_f on the grain size using the Williamson-Hall technique [13-14] by XRD. In Fig. 7, a typical XRD chart of the nickel thin film having 1 μm in thickness shows diffraction peaks of nickel comprising (111), (200), (220), and (311) diffraction. In the Williamson-Hall technique, the line broadening, β of a Bragg diffraction angle θ_B originating from a small crystalline grain size d and strain ε in a film is given by

$$\beta \cos \theta_B = \frac{K\lambda}{d} + 4\varepsilon \sin \theta_B, \tag{6}$$

where K is the shape factor and λ is the X-ray wavelength. To calculate β from the profile of diffraction peak, the following Gaussian function $G(\theta)$ was used as a fitting function for the diffraction peak,

$$G(\theta) = \frac{(L_{\max} - L_{\text{back}})}{\Gamma^2 + (\theta - \theta_c)^2} + L_{\text{back}}, \tag{7}$$

where Γ is the fitting parameter, L_{\max} is the peak intensity of diffraction, L_{back} is the intensity of background, θ_c is the center value of the diffraction peak. Using the integral breadth, the line broadening β for the (hkl) plane diffraction is equal to πL . The conventional Williamson-Hall plot is shown in Fig. 7 (b).

The value of K is in a range of 0.89 to 1.3, which is dependent on the shape of grain [21]. Assuming that the grains in the Ni thin film have a sphere and the diffraction peak can be approximately represented by the Gaussian function, we can use $K=1$. In Fig. 7 (b), the y-section of the straight line on which all the data almost lies gives the mean grain size, d according to Eq. (6).

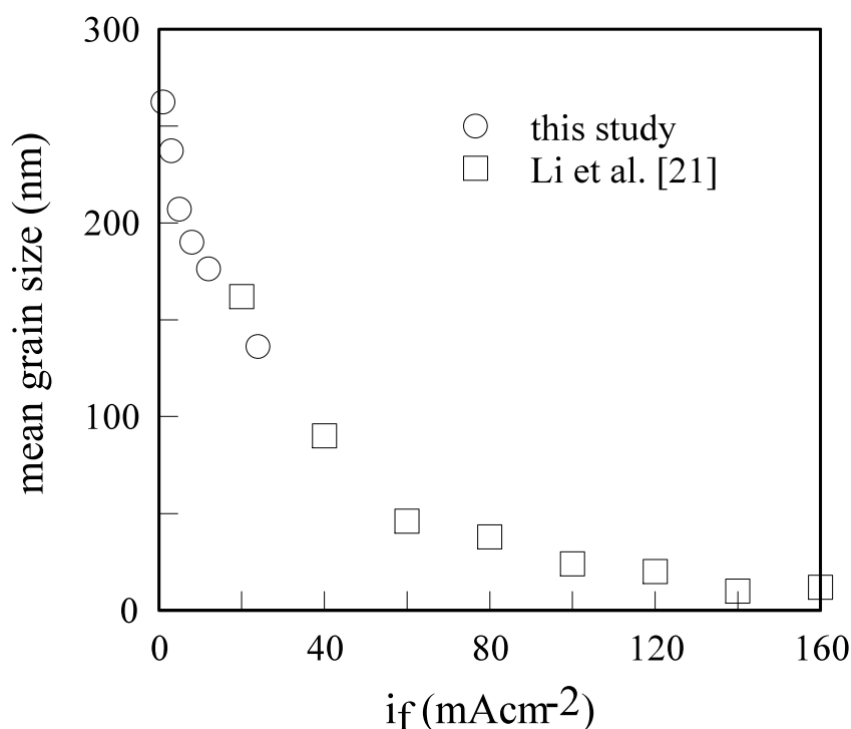


Figure 8. A plot of the mean grain size vs. the Faradaic current pulse amplitude i_f in the nickel thin film electrodeposited at an on-time of 5 ms and an off-time of 5 ms.

In Fig. 8, the grain size decreases with the amplitude of the faradaic current pulse i_f . The grain size in Ni-Co films [22] electrodeposited by a current pulse technique is shown as a reference, which also indicates a decrease in the mean grain size with the amplitude of the current pulse. The decrease in the grain size in pulse electrodeposition may be qualitatively explained by a decrease in the diffusion length [23] $l_d = (D/F)^\psi$ or a decrease in the critical island size [24-25] $L_c \propto F^{-\psi}$ where F is the average number of ions arriving at the electrode, D the diffusion coefficient of adatoms, and ψ an exponent dependent on the mechanism of grain formation. The increase in the amplitude that lessens l_d and L_c increases the internal stress. This also shows the internal stress combined with the surface topography.

In this study, no additive was added to the solution. Saccharin sodium used for a typical additive in the electrolyte is expected to have an effect of pinning or depinning a moving interface at active sites in the interface. Within a framework of the dynamic scaling theory, the effect is called as a quenched noise. In a further study, the effect of saccharin sodium that causes a decrease in the internal stress and a shift from the tensile to the compressive stress will be treated as a quenched noise that causes a deviation from the scaling law.

4. CONCLUSIONS

We have investigated the internal stress in rectangular current pulse electrodeposition using the bent strip measurement. The internal stress is found to be described by the power law $\sigma \sim h^{-0.24} \left[i_f \left(\frac{T_{on}}{T_{on} + T_{off}} \right) \right]^{0.74}$. The scaling behavior of the internal stress suggests that the internal stress links the surface topography determined by the surface roughness and the grain size.

ACKNOWLEDGEMENTS

This work is supported by Grant-in-Aid for Scientific Research (C), No. 22560025 by the Ministry of Education, Science, and Culture of Japan. The author deeply appreciates Mr. M. Z. Azmir, Mr. R. Firdaus, and Mr. M. Tokuzato for their help in the experiments.

References

1. G. C. A. M. Janssen, *Thin Solid Films*, 515 (2007) 6654.
2. P. J. Withers and H. K. Bhadeshia, *Mater. Sci Technol.*, 17 (2001) 365.
3. J. J. Kelly, S. H. Goods, A. A. Talin, and J. H. Hachman, *J. Electrochem. Soc.*, 153 (2006) C318.
4. G. C. A. M. Janssen, *Appl. Phys. Lett.*, 85 (2004) 3086.
5. N. Goldenfield, *Lectures on Phase Transitions and Renormalization Group*, Prerusus Book, Massachusetts, 1992.
6. A-L. Barabási and H. E. Stanley, *Fractal Concepts in Surface Growth*, Cambridge Uni. Pr., New York, 1995.
7. S. G. Mayer and K. Samwer, *Phys. Rev. Lett.*, 87 (2001) 036105.
8. N. Ibl, *Surf. Technol.*, 10 (1980) 81.
9. D. Xu, V. Sriram, V. Ozolins, J-M. Yang, K. N. Tu, G. R. Stafford, and C. Beauchamp, *J. Appl. Phys.*, 105 (2009) 023521.

10. K. Schuler, B. Philippi, M. Weinmann, V. M. Marx, and H. Vehoff, *Acta Materialia*, 61 (2013) 3945.
11. M. Saitou, *J. Appl. Phys.*, 106 (2009) 034917.
12. J. J. Kelly, N. Yang, T. Headley, and J. Hachman, *J. Electrochem. Soc.*, 150 (2003) C445.
13. M. Birkholz, *Thin Film Analysis by X-Ray Scattering*, Wiley-VCH, Weinheim, 2006.
14. V. Biju, N. Sugathan, V. Vrinda, and S. L. Salini, *J. Mater. Sci.*, 43 (2008) 1175.
15. G. C. A. M. Janssen, F. D. Tichelaar, and C. C. G. Visser, *J. Appl. Phys.*, 100 (2006) 093512.
16. D. E. Wolf and J. Villatin, *Europhys. Lett.*, 13 (1990) 389.
17. K. Schuler, B. Philippi, M. Weinman, V. M. Marx, and H. Vehoff, *Acta Mater.*, 61 (2013) 3945.
18. P. Leisner, C. D. Zanella, I. Belov, C. Edström, and H. Wang, *Trans. Int. Met. Finish.*, 92 (2014) 336.
19. L. P. Bicelli, B. Bozzini, C. Mele, and L. D'Urzo, *Int. J. Electrochem. Sci.*, 3 (2008) 356.
20. A. Bhandari, S. J. Hearne, B. W. Sheldon, and S. K. Soni, *J. Electrochem. Soc.*, 156 (2009) D279.
21. J. I. Langford and A. J. C. Wilson, *J. Appl. Cryst.*, 11 (1978) 102.
22. Y.D. Li, H. Jiang, W. Huang, and H. Tian, *Appl. Surf. Sci.*, 254 (2008) 6865.
23. P. Jensen, A. -L. Barabási, H. Larralde, S. Havlin, and H. E. Stanley, *Phys. Rev. E*, 50 (1994) 618.
24. J. Rottlerand and P. Maas, *Phys. Rev. Lett.*, 83 (1999) 3490.
25. J. Krug, P. Politi, and T. Michely, *Phys. Rev. B*, 61 (2000) 14037.

© 2015 The Authors. Published by ESG (www.electrochemsci.org). This article is an open access article distributed under the terms and conditions of the Creative Commons Attribution license (<http://creativecommons.org/licenses/by/4.0/>).